A Second Role for the Second Messenger Cyclic-di-GMP in *E. coli*: Arresting Cell Growth by Altering Metabolic Flow

YuneSahng Hwang and Rasika M. Harshey*

Department of Molecular Biosciences

University of Texas at Austin

Austin, TX 78712

*Correspondence to: rasika@austin.utexas.edu

Running title: A second role for the second messenger c-di-GMP

Abstract

Cyclic-di-GMP primarily controls motile to sessile transitions in bacteria. Diguanylate cyclases (DGCs) catalyze the synthesis of c-di-GMP from two GTP molecules. Typically, bacteria encode multiple DGCs that are activated by specific environmental signals. Their catalytic activity is modulated by c-di-GMP binding to autoinhibitory sites (I-sites). YfiN is a conserved inner membrane DGC that lacks these sites. Instead, YfiN activity is directly repressed by periplasmic YfiR, which is inactivated by redox stress. In *E. coli*, an additional envelope stress causes YfiN to relocate to the mid-cell to inhibit cell division by interacting with the division machinery. Here, we report a third activity for YfiN in *E. coli*, where cell growth is inhibited without YfiN relocating to the division site. This action of YfiN is only observed when the bacteria are cultured on gluconeogenic carbon sources, and is dependent on absence of the autoinhibitory sites. Restoration of I-site function relieves the growth-arrest phenotype, and disabling this function in a heterologous DGC causes acquisition of this phenotype. Arrested cells are tolerant to a wide range of antibiotics. We show that the likely cause of growth arrest is depletion of cellular GTP from run-away synthesis of c-di-GMP, explaining the dependence of growth arrest on gluconeogenic carbon sources that exhaust more GTP during production of glucose. This is the first report of c-di-GMP-mediated growth arrest by altering metabolic flow.

Significance

The c-di-GMP signaling network in bacteria not only controls a variety of cellular processes such as motility, biofilms, cell development and virulence, but does so by a dizzying array of mechanisms. The DGC YfiN singularly represents the versatility of this network in that it not only inhibits motility and promotes biofilms, but also arrests growth in *E. coli* by relocating to the mid-cell and blocking cell division. The work described here reveals that YfiN arrests growth by yet another mechanism in *E. coli* – changing metabolic flow. This function of YfiN, or of DGCs without autoinhibitory I-sites, may contribute to antibiotic tolerant persisters in relevant niches such as the gut where gluconeogenic sugars are found.

Introduction

Bacteria show a remarkable ability to adapt to different environmental conditions through multiple signaling networks [1, 2]. Some of these networks commonly use cyclic or linear nucleotides to link environmental stimuli to specific bacterial responses [3, 4]. Cyclic di-GMP (c-di-GMP) was first identified in *Gluconacetobacter xylinus* for its role in cellulose production [5]. In most bacteria c-di-GMP controls the transition between motile and sessile behaviors, but is not limited to these functions [6, 7]. Broader roles for this system include virulence, progression through the cell cycle, phage resistance, and surface attachment [8-11].

Intracellular c-di-GMP levels are regulated by multiple diguanylate cyclases (DGCs) identifiable by a signature GGDEF active-site (referred to as GGDEF domain) that catalyze the synthesis of c-di-GMP from two GTP molecules, and multiple phosphodiesterases (PDEs) identifiable by EAL or HD-GYP domains that break down c-di-GMP first to linear pGpG and subsequently to GMP [12, 13]. Although ectopic expression of most DGCs and PDEs often leads to dramatic phenotypes, their native expression often does not, as observed by lack of an observable phenotype when their genes are experimentally mutated, indicating that these enzymes may be only activated under specific environmental conditions. The presence of specific sensory modules such as HAMP, PAS, LuxR or BLUF domains allows these enzymes to respond to a variety of sensory cues, both chemical and physical; however, most signals activating these enzymes are still unknown [14-18]. The c-di-GMP produced in response to these signals elicits its varied outputs primarily by binding to cellular effectors and targets.

DGCs are regulated not only by environmental signals but can also self-regulate. An autoinhibition (I) site located close to the active site was first identified in the DGC PleD of *Caulobacter crescentus*, where it regulates enzyme activity through negative feed-back, curtailing excess c-di-GMP production [12]. This site (primary I site; I_p) is identifiable by an RXXD consensus located five amino acids upstream of the GGDEF motif. c-di-GMP bound at I_p causes a conformation change that leads to the repression of enzymatic activity; accordingly, mutations in conserved I_p residues increase c-di-GMP production [12]. Based on structural

studies, additional ariginine residues located outside the GGDEF domain in PleD were also seen to contribute to the c-di-GMP pocket for feedback inhibition; these were designated the secondary I site (I_s) [19]. A different role for I_s was reported for the DGC GcbC in *Pseudomonas fluorescens*, where this site is required for interaction of GcbC with its target protein LapD, which controls biofilm production [20].

YfiN, also called DgcN or TpbB, is a conserved inner membrane DGC with a Per-Arnt-Sim (PAS)-like sensory domain in the periplasm and HAMP-GGDEF domains in the cytoplasm [21, 22]. *E. coli* YfiN lacks both I_p and I_s sites, as do the majority of bacterial YfiN homologs. In *E. coli, Salmonella enterica* and *Pseudomonas aeruginosa*, the enzymatic activity of YfiN is repressed by periplasmic YfiR [16, 23, 24]. Redox stress can cause YfiR to dissociate from YfiN, activating its DGC function [16, 24]. In *P. aeruginosa*, transposon disruption of *yfiR* led to increased biofilm formation through the Pel/Psl biosynthesis pathway, and enzymatically inactive YfiN showed less virulence in the mouse model compared to wild-type (WT) [16]. YfiN was also shown to be important for biofilm maintenance in response to peroxide stress in *P. aeruginosa* [25].

In *E. coli*, YfiN exhibits the canonical motility-inhibition function of a DGC [24]. A second very different function for YfiN is a two-step response to redox and envelope stresses: in response to redox stress YfiN produces c-di-GMP, and in response to a second envelope stress YfiN moves to the mid-cell to arrest cell division [24]. Unlike known cell division inhibitors [26], the interaction of YfiN with cell division proteins FtsZ and ZipA retains the Z ring at the mid-cell but prevents septal invagination [24]. We report here a third function for YfiN in *E. coli,* where YfiN arrests growth by a mechanism different from cell division arrest. This mechanism exploits the absence of regulatory I sites in this DGC. We show that when growing on gluconeogenic sugars, unregulated c-di-GMP synthesis by YfiN depletes cellular GTP, which is the likely cause of failure of all macromolecular synthesis. Growth arrest can be reversed by reintroducing the I sites. Such a function for a DGC has not been previously reported in bacteria. This ability of YfiN to enable survival by shutting down growth, allows the bacteria to

tolerate a broad spectrum of antibiotics.

Results

YfiN arrests *E. coli* growth on specific carbon sources

Prior studies conducted in *E. coli* growing in LB with ectopically expressed YfiN reported that even though expression was induced from the beginning of a growth cycle, YfiN appeared at the division site just prior to the onset of the stationary phase, resulting in cell division arrest [24]. When cells were grown in minimal M9 glycerol however, we observed that irrespective of whether the ectopic expression was from a plasmid (pYfiN; PBAD promoter) or from its chromosomal location (cYfiN; PTrc promoter), growth began to slow as early as two hours post-YfiN induction and to remain arrested (**Fig. 1A, B**). The DGC function of YfiN was important for this phenotype, as observed by lack of growth arrest in the active site mutant pYfiN(GGAAF), where the GGDEF signature motif is changed to GGAAF **(Fig. 1C**).

To test whether localization of YfiN to the mid-cell is required for the growth arrest observed in Figure 1 (**A,B**), the location of both $cYfiN_{GFP}$ and $pYfiN_{GFP}$ was monitored in M9 media. $cYfiN_{GFP}$ was found dispersed throughout the cell, while $pYfiN_{GFP}$ relocated to the mid-cell in 60% of the cells (**Fig. 2A**). Thus, the observed growth-arrest by cYfiN is not related to its ability to localize at the division site, while that of pYfiN may include division arrest (**Fig. 1A, B**). To investigate if the mid-cell localization of pYfiN in 60% of the cells was related to the higher expression levels from a plasmid, we monitored the behavior of a plasmid encoded R260A mutant of YfiN (R260 is located in the cytoplasmic domain) that does not localize to the mid-cell (**Fig. 2B**). Like pYfiN, pYfiN(R260A) induction resulted in severe motility inhibition on soft agar plates, indicating robust c-di-GMP production (**Fig. 2C**). Despite its failure to localize to the mid-cell, the R260A mutant arrested growth similar to WT YfiN (**Fig. 2D**). We conclude that the inability to grow in M9 glycerol is a new phenotype of YfiN, distinct from its

ability to arrest cell division by interacting with the divisome at the mid-cell.

E. coli has 12 DGCs, of which five (including YfiN) harbor a transmembrane region. To test if this new phenotype of YfiN is related to its membrane location, and to also control for overexpression artifacts, we cloned the other four transmembrane DGCs (C, E, F and J) [27] under PBAD control. In contrast to YfiN, none of these four DGCs arrested growth in M9 glycerol (**Fig. 1D**). Except for DgcF, the ectopic expression of DgcC, E and J inhibited motility, suggesting that they were active as DGCs (**Fig. 2E)**. We conclude that early growth arrest in M9 glycerol is unique to YfiN.

A clear difference between the early growth-arrest observed in this study (**Fig. 1A,B**) and the late growth-arrest phenotype of YfiN reported earlier [24] was the growth medium: minimal M9 glycerol in the present study, and nutrient-rich LB in the earlier one. When glycerol was substituted with glucose, the most favored carbon source for *E. coli*, cYfiN no longer inhibited growth in the M9 medium (**Fig. 1E**, third set of bars from the left). In *E. coli* growing aerobically, glucose is directly integrated into glycolysis as glucose 6-phosphate (G6P) and consumed through the tricarboxylic acid cycle (TCA), while glycerol, an energy-poor carbon source is incorporated into central metabolism as dihydroxyacetone phosphate (DHAP), a metabolite that can participate in both gluconeogenic and glycolytic processes [28] (**Fig. 1F**). To explore this finding further, we provided several gluconeogenic and non-gluconeogenic substrates as carbon sources in the M9 medium. For the former we chose G6P, lactose, glucose and arabinose, and for the latter we chose the following: sugar alcohols in addition to glycerol (sorbitol, mannitol), various other sugars (fructose, mannose, maltose), acetate, and TCA cycle intermediates (pyruvate, succinate). There was a clear-cut difference in the ability of YfiN to arrest growth on the two sets of carbon sources, which was patterned after the glycerol and glucose examples i.e. only gluconeogenic sugars arrested growth. If the differential growth arrest phenotype of YfiN on these two types of substrates is because of the higher energy produced by one substrate type versus the other, the expectation is that providing both substrates would override the effect of the gluconeogenic substrate. This was

found to be the case (**Fig. S1A-D**). To test whether YfiN-mediated growth arrest is reversible, either glucose or LB was added 2 hours post-induction of YfiN. Bacteria resumed growth immediately, suggesting that YfiN-mediated growth arrest is fully reversible and that cells are not dead (**Fig. S1E**).

Growth arrest is correlated with absence of autoinhibitory I sites in YfiN

Given that the DGC activity of YfiN is required to mediate growth arrest (**Fig. 1C**), we first tested whether the canonical function of c-di-GMP (turning on biofilm pathways / shutting down motility) played a role. This was done in two ways: 1) simultaneous expression of YfiN with YhjH (the most active PDE in *E. coli*) expected to degrade c-di-GMP and 2) disruption of six key genes that control the major biofilm pathways in *E. coli* (production of cellulose, PGA, colanic acid, Type 1 fimbriae, EPS etc.) [29]. The inhibitory effect of YfiN on motility was substantially relieved in the first case, showing that c-di-GMP levels were reduced as expected (**Fig. S2A**), and biofilm levels decreased in the second case (**Fig. S2C**). However, neither manipulation changed the growth arrest pattern (**Fig. S2 B,D**), eliminating the possibility that the canonical functions of c-di-GMP contribute to the observed growth arrest phenotype of YfiN.

In thinking about what distinguishes YfiN from the all the other *E. coli* DGCs previously tested (Dgc C, E, F, J), we noted that YfiN lacks the consensus autoinhibitory I site residues (I_p and I_s), which bind c-di-GMP to feedback regulate enzyme activity (**Fig. 3AB**) [12, 30]. We reasoned that lack of autoregulation would lead to continual c-di-GMP production, hence depletion of cellular GTP. Depletion of GTP as a mechanism of growth arrest is well-established in the (p)pGpp-mediated pathway [31]. Imbalance in nucleotide pools is also known to disrupt growth [32, 33]. To test the GTP depletion idea, we rebuilt the two YfiN I sites (I_p and I_s) both sequentially and together. I_p was restored by changing GLRH to the consensus RXXD, and I_s by changing N280 to R. Only when both I sites were reconstituted, was growth

arrest fully reversed (**Fig. 3C**). These changes did not perturb the DGC activity of the I-site reconstituted strains as monitored by motility inhibition in soft agar plates (**Fig. 3D**). To test this idea further, we mutated the I_p site (RESD → GESD) in DgcA, a robust heterologous DGC from *C. crescentus* [12]. Expression of WT DgcA in *E. coli* did not elicit growth arrest in M9, but expression of the DgcA I_p mutant did (**Fig. 3E**). Thus, both loss of the growth-arrest phenotype in YfiN, and gain of this phenotype by DgcA by merely restoring and inactivating I-site function, respectively, allows us to conclude that unregulated c-di-GMP production is responsible for the arrest, not by increasing c-di-GMP levels per se (see **Fig. S2B**), but likely by depleting cellular GTP levels.

YfiN expression depletes intracellular GTP

To test our conjecture that GTP depletion due to unregulated c-di-GMP synthesis is the cause of growth arrest by YfiN, we first compared cellular nucleotide levels with (+) or without (-) induction of cYfiN by metabolomic analysis of a standard panel of 219 intracellular metabolites. Of these, the levels of five ribonucleotides relevant to this study are shown in **Figure 4AB**. c-di-GMP levels were high in the cYfiN+ strain as expected. A consistent decrease in the levels of GTP, ATP, UTP and CTP was seen in experimental samples compared to the controls. To confirm the drop in GTP concentration upon YfiN expression, we next used a luciferase-linked GTP assay (GTPase-Glo™), which converts GTP into ATP, the latter detected by the light produced by the luciferase reaction (**Fig. 4C**)**.** We observed a 50% decrease in GTP levels in YfiN-expressing cells, supporting the GTP metabolomics data. To monitor GTP levels by a third method, as well as to test the proficiency of various YfiN I-site mutants in converting GTP to c-di-GMP, cell lysates expressing pYfiN and its I-site double mutant (I_{ps}) variant were incubated with [α-^{32}P] GTP at regular time intervals from 0-15 min and the products analyzed by thin layer chromatography (TLC); only data for the 10 min time point are shown because in this experiment, WT pYfiN lysates depleted almost all of the input GTP at this time, while ~20% of input GTP still remained in the I_{ps} mutant (**Fig. 4D**). We then compared the time course of

GTP consumption by WT pYfiN with that of I-site regulated pDgcA (**Fig. 4E**). By16 min, YfiN had consumed most of the GTP, while half of the input GTP still remained during DgcA expression. This difference in enzymatic activity may be critical when intracellular GTP is low to begin with in glycerol-fed cells (~2.5 fold lower compared to glucose) [39]. We finally used a fourth method to verify GTP depletion by quantifying the absolute levels of GTP using mass spec as described under Methods. GTP levels decreased significantly in cells expressing pYfiN (**Fig. 4F**). Although $_{p}$YfiN(I_{ps}) and $_{p}$DgcA cells showed higher levels of GTP compared to $_{p}$EmptyVector, the difference was not statistically significant. Thus, four different kinds of measurements show that YfiN expression depletes cellular GTP as expected. The data in Fig. 4B show that YfiN expression impacts all ribonucleotide triphosphate levels as well.

An alternative explanation for the depletion of cellular GTP observed in Figure 4 could be activation of the (p)ppGpp synthesis pathway, during which a diphosphate from ATP is transferred to the 3′-OH oxygen of GTP/GDP; (p)ppGpp is the primary regulator of GTP homeostasis in *E. coli* [34], and deployed in bacteria experiencing various stresses [35, 36]. In *E. coli*, RelA and SpoT are the only known enzymes that synthesize as well as degrade (p)ppGpp, which is not made in the absence of both proteins (ppGpp^{0}) [37]. To test this alternate explanation, we induced YfiN in *ΔrelA* or *ΔrelAΔspoT*(ppGpp^{0}) background, expected to have minimal amounts of (p)ppGpp. Both mutant strains showed growth arrest as early as 2 hours after induction of YfiN (**Fig. S3**), ruling out involvement of (p)ppGpp in YfiN-induced arrest.

To run an independent check of studies concluding that less GTP is available during growth on poor carbon sources such as glycerol and acetate [38], we considered tweaking enzymes contributing to gluconeogenesis. We chose phosphoenolpyruvate carboxy kinase (PCK) for our test, as it mediates an irreversible step in the pathway, converting oxaloacetate to phosphoenolpyruvate, and promotes gluconeogenesis [39] (**Fig. S4A**). Increasing PCK levels might therefore be expected to increase severity of the growth arrest. We monitored growth in M9 mannitol, where YfiN-mediated growth arrest is not as severe as in M9 glycerol

(**Fig. 1E**). In this growth medium, PCK induction resulted a severity of growth arrest similar to that seen in M9 glycerol (**Fig. S4B)**. These data, along with those demonstrating that YfiN-mediated growth arrest can be reversed by the addition of a non-gluconeogenic sugar (**Fig. S1E**), support our hypothesis that the availability of GTP pools underlies the mechanism of the YfiN growth arrest.

In summary, we infer from the data in this and prior sections that absence of feed-back control of c-di-GMP synthesis in YfiN, combined with the energy-expensive metabolism of gluconeogenic sugars, deplete cellular GTP to levels unsustainable for growth, which can be rescued by utilizing non-gluconeogenic sugars.

YfiN-arrested cells are tolerant to a broad class of antibiotics

To investigate whether all major cellular processes - cell wall, protein and DNA synthesis – are arrested by YfiN during growth on M9 glycerol, we exposed cells to the antibiotics Ampicillin, Gentamicin, and Ciprofloxacin, [40]. At the bactericidal concentrations used, $_{c}$YfiN-expressing cells survived better than control cells in the presence of all three antibiotics when tested as follows. Cells were first grown on M9 glycerol + antibiotic plates for 12 hours (**Fig. 5A,** middle). They were then transferred with an inoculation loop to LB plates without added antibiotics for recovery (**Fig. 5A,** right; Gen/Amp/Cip stamps only point to the antibiotic condition from where cells were taken). The results are shown in **Figure 5B** (note again that there are no antibiotics in these plates, as illustrated in Fig. 5A, right). Without YfiN expression, cells succumbed to all three antibiotics they were initially plated on, as judged by loss of recovery of viable cells (**Fig. 5B, left**); this was not the case when YfiN was expressed (**Fig. 5B, right**). To quantify the number of YfiN-expressing cells that survive antibiotic treatment, a similar assay was performed in a M9 glycerol liquid media, where after 4 hours of antibiotic exposure, survival was measured by CFU counts on LB plates (**Fig. 5C, D**). The results were similar to those reported in Fig. 5B. We conclude that YfiN effectively shuts down all major cellular processes

in M9 glycerol.

Since the enzymatic function of YfiN is closely related to the growth arrest phenotype, we reasoned that it should also be linked to its antibiotic tolerance property. This was tested in two ways using $_{c}$YfiN – by concomitantly increasing the expression of its periplasmic inhibitor YfiR (pYfiR) (**Fig. S5A**), as well as by testing the GGDEF active site mutant (**Fig. S5B**). Both manipulations abrogated the antibiotic (Cip) tolerance phenotype. We conclude that the DGC activity of YfiN mediates both growth arrest and antibiotic tolerance.

Native YfiN delays exit from lag phase during exponential growth

The results presented thus far have relied on ectopic expression of YfiN. To test if YfiN expressed from its native chromosomal promoter contributes to antibiotic tolerance, we used overnight cultures of WT and *ΔyfiN* strains grown in LB to inoculate fresh media - either M9 glycerol or glucose - and sampled them over the time course of growth for their ability to survive a 4-hour exposure to Ampicillin. In M9 glycerol, WT grew slower than *ΔyfiN* as measured by OD_{600}, this difference in growth was not observed in glucose (**Fig. 6A, B**). Using CFU counts from the same experiments, we calculated the doubling time of the two strains along the growth curve at 2 hour intervals (figure insets) and observed that in M9 glycerol, both strains were still in the lag phase in the first interval (0-2 hour) but that in the next interval (2-4 hour), WT showed a higher doubling time and hence a delayed transition to exponential phase compared to *ΔyfiN* (**Fig.6A,** inset); this delay was not observed in glucose (**Fig.6B,** inset). We note that the doubling time of both strains were similar during the exponential phase in M9, so the apparently overall slower growth of the WT strain is due to growth delay only at early times. Survival in Ampicillin along the time course (**Fig. 6CD**) could be superimposed on the data in Fig. 6AB: WT survived better than Δ*yfiN* after antibiotic treatment only in the lag phase and only in M9 glycerol (compare **Fig. 6C** and **Fig. 6D**). This survival advantage of WT

over *ΔyfiN* during the lag phase may be explained by the reported sharp initial increase of YfiN when overnight cultures are inoculated into fresh media [41].

In summary, the growth delay/arrest property of YfiN is seen even when the protein is expressed from its native chromosomal location.

Discussion

Cyclic-di-GMP is the most ubiquitous signaling nucleotide in bacteria, with dozens of DGCs involved in its production. These enzymes enable a variety of downstream outputs. In this study, we have discovered a new output for the DGC YfiN, made possible by a particular structural feature of the enzyme that restricts growth in specific nutrient conditions, allowing *E. coli* to survive through stressors like antibiotics.

YfiN exploits the absence of autoinhibitory I sites to enable a novel mode of survival

I sites (I_p-I_s) are common in DGCs, and serve an important role in binding c-di-GMP to feed-back regulate DGC activity [12, 20], thus controlling the amount of c-di-GMP available to bind to downstream effector proteins. YfiN belongs to a small fraction of DGCs in *E. coli* (3/12, based on sequence gazing) that do not encode these sites. Absence of this regulatory structural feature appears to be the hallmark of the majority (>90%) of all bacterial YfiN homologs found in the UniProt database. YfiN activity is instead controlled by the periplasmic repressor YfiR, known to be inactivated by redox stress [16, 24]. Given that YfiN is the most robust DGC in *E. coli* [24], we suspect other periplasmic stresses that unfold proteins may also activate this enzyme [42]. Once activated, one would not expect YfiN to stop c-di-GMP synthesis until the inducing stressors are gone. We show in this study that unregulated c-di-GMP production comes with a metabolic cost. The nature of this cost came to the fore when *E. coli* grown on gluconeogenic carbon sources such as glycerol, mannitol, or sorbitol were

observed to arrest cell growth, a phenotype that required the DGC activity of YfiN (**Fig. 1**), but did not require its relocation to the cell division site at the mid-cell (**Fig. 2**). That it was the unregulated DGC activity of YfiN that was responsible for growth arrest was established by reconstituting the consensus sequence of both I_p and I_s sites, which restored growth (**Fig. 3C**). Conversely, inactivating the I_p site of DgcA from *C. cresentus*, conferred on it the growth arrest phenotype (**Fig. 3D**). We note that WT DgcA inhibits *E. coli* motility more strongly than YfiN (**Fig. 3E**), suggesting that DgcA generates higher steady state levels of c-di-GMP, yet fails to arrest growth. Thus, it is not the c-di-GMP concentration per se, but rather its unchecked synthesis that is responsible for arresting growth (see **Fig. S2B**).

A second function for I_s in interacting with a downstream effector protein was seen in *P. aeruginosa* [20]. One could argue that introducing mutations around the I-site of YfiN disrupted interaction with a binding partner, which is responsible for the growth arrest. This is unlikely because the heterologous DgcA, which is not expected to have a binding partner in *E. coli*, acquired this phenotype by reverse mutations at similar positions.

The studies described above were performed under ectopic expression of YfiN alone, in order to mimic conditions where YfiR is non-functional. We imagine that a combination of periplasmic stress plus the stress of growing on energetically costly substrates might create fertile grounds for growth arrest in natural habitats of YfiN-expressing *E. coli*. That this arrest is reversible, as seen by revival of growth upon adding non-gluconeogenic sugars (**Fig. S1E**), suggests that *E. coli* employs YfiN to weather inhospitable conditions. A reversible quiescent state is known to favor adaptive evolution from microbes to humans [43-45]. Our findings likely extend to all YfiN-encoding bacteria given that the majority of the homologs lack the I_p site. In those that do have this site (*Pseudomonas* and *Yersinia* species), the I_s site is absent (Fig. S6). In light of our data showing that both I sites are required to relieve growth arrest (**Fig. 3C**), feed-back inhibition of YfiN activity is likely inefficient in the bacteria harboring only the I_p site [21, 22].

YfiN activity during growth on gluconeogenic carbon sources depletes cellular GTP

The clear distinction between gluconeogenic and glycolytic carbon sources in promoting growth arrest by YfiN is striking (**Fig. 1E**). Gluconeogenesis is the process by which cells synthesize glucose 6-phosphate from non-hexose sugars [46]. While eukaryotic cells as well as other bacteria consume both ATP and GTP in this process, *E. coli* is known to only consume ATP [47]. Each cycle of gluconeogenesis requires 4 ATPs plus 2 NADHs, resulting in net deficit of 9 ATPs. Lower levels of ATP will consequently lower those of GTP, since the γ phosphate of ATP is used by nucleoside diphosphate kinase (ndk) to synthesize GTP from GDP [48] (**Fig 7**). In glycerol, there is less ATP produced during TCA cycle as well (20 ATPs compared to 36~38 ATPs in glucose). Indeed, *E. coli* grown in M9 glycerol and acetate has been demonstrated to have less intracellular ATP/GTP than in glucose [38]. Unregulated consumption of GTP by YfiN will further increase cellular metabolic stress under these conditions. The lower cellular GTP levels we see upon induction of YfiN during growth on M9 glycerol are therefore expected (**Fig. 4A**). Lowering GTP levels even by two-fold (**Fig. 4B,C,F**) should be sufficient to arrest growth given *in vitro* data showing that the transcription rate from a ribosomal RNA promoter (*rrnB*) is highly sensitive to GTP concentrations [49]. In the ecological niches that heterotrophic bacteria inhabit, they obtain carbon from dissolved organic matter. Although *E. coli* is primarily a commensal of mammals, and to a lesser extent birds, it can be isolated from a variety of host species as well as soil, sediments, and water. We imagine that the particular YfiN function we have uncovered in this study may manifest in certain ecological niches rich in gluconeogenic sugars or in non-carbohydrate substrates not tested in this study. For example, each part of the human gut has different concentrations of carbon sources and types [50].

In summary, we conclude that uncontrolled synthesis of c-di-GMP by YfiN is the proximate cause of depletion of cellular GTP. These nucleotides are essential for the synthesis of the major cellular macromolecules DNA, RNA and protein, explaining why cells enter growth arrest when using the energetically more costly gluconeogenic carbon sources for synthesis

of glucose-6-P.

YfiN contributes to increased tolerance to antibiotics

YfiN is known to inhibit cell division in response to redox and envelope stresses, and to protect *E. coli* from envelope-disrupting environments when ectopically expressed [24]. We show here that ectopic expression of YfiN in M9 glycerol also increases tolerance to a broad class of antibiotics such as Ampicillin, Gentamicin, and Ciprofloxacin, which target and disrupt a variety of cellular processes (**Fig. 5**). This function of YfiN is related to its unregulated DGC activity (**Fig. 1C, 3C, S5**). Bacteria are continuously exposed to environmental stresses and knowing when to stop proliferating is key to their survival. Surprisingly, even in the absence of overt stress, we observed that native YfiN confers a significant advantage by delaying the exit of cells from the initial lag phase of growth, a phenotype again only observed in minimal M9 glycerol media (**Fig. 6CD)**. Although it may seem counter-intuitive to harbor a gene preventing bacteria from proliferating, persisting in the lag phase may help bacteria in transitioning to a new environment, particularly if the environment is stressful or nutrients are scarce. An increase in the lag phase has been reported as an integral step for developing antibiotic resistance [51, 52]. It has been suggested that a prolonged lag could buy the bacteria time to diversify adaptive phenotypes [53, 54]. The increased survival advantage of WT compared to *ΔyfiN*, supports this concept (**Fig. 6AB**). The importance of the lag phase is not limited to surviving antibiotic stress alone. A transcriptional profiling study of *S. enterica* showed that genes associated with DNA repair and protein degradation were induced during lag phase, implicating a crucial role for this phase in repairing damaged cellular components [52, 55]. Bacteria are also known to reorganize their metabolism during the lag phase to achieve optimal growth [55], and two distinct lag phases were observed in *E. coli* supplied with arabinose [56]. Thus, by regulating the duration of the lag phase, we suspect that YfiN not only confers increased tolerance to antibiotics but also other advantages such as optimizing

DNA repair and metabolic pathways for growth. The mechanism of how YfiN selectively halts the growth during the lag phase is still under the study.

Coda. YfiN seems to have emerged as a DGC that responds multiple metabolic stresses – redox, envelope, gluconeogenic substrates – and has thus far shown multiple output responses designed to hunker down, make biofilms, and persist.

Materials and Methods

Strains, growth conditions, mutagenesis, and plasmid constructions. Strains and plasmids used in this study are listed in Table S1. The WT parent strain for *E. coli* was MG1655 for all experiments. All strains were grown in M9M (M9 minimal media + 0.2% glycerol + 0.2% casamino acid) or in LB broth (10 g/liter tryptone, 5 g/liter yeast extract, 5 g/liter NaCl) unless noted otherwise. When appropriate, the following antibiotics were used: Ampicillin (100 µg/ml), Chloramphenicol (20 µg/ml), Kanamycin (50 µg/ml), and Gentamicin (30 µg/ml). For inducible plasmids, 100µM isopropyl-β-d-thiogalactopyranoside (IPTG) or 0.02%(w/v) L-arabinose were added as indicated in the figures or legends. To monitor the growth of cells, optical density was measured at the wavelength of 600nm (OD_{600})

HK 533 strain was constructed similarly to HK532 strain [24]. Using lambda red recombination [57], *yfiR* was replaced with PTrc promoter and a kanamycin cassette inserted in an orientation opposite to the direction (←) of *yfi* operon transcription, in order to prevent polar effects on *yfiN* expression.

For cloning of expression plasmids, gene sequences were amplified from the genomic DNA of WT strains by using PCR and introduced into pBAD30, pBAD33.

To restore or introduce I-sites, specific primers designed for single base pair substitutions were used for PCR amplification using pBAD_YfiN or DgcA as templates. Following amplification, the original templates were digested with 1 unit of DpnI and PCR products were used for transformation and selection.

All constructs were confirmed by DNA sequencing.

Recovery assay. For the experiment shown in Fig. S1E, cYfiN strain was propagated in M9M with IPTG for induction. After 2 hours post-induction, 0.2% glucose was added for recovery, followed by measurement of OD_{600} every 2 hours.

Motility assay. LB soft agar or swim plates were made using 0.3% Fisher agar. 5 µl of an

overnight culture was inoculated in the center and plates incubated at 30°C for 8-12 hours. Swim ring diameter was measured to compare motility across strains.

Biofilm assay. Cells were propagated in M9M in 96-well plates. After 20 hour incubation at 37℃, plates were washed twice with water and dried for 2 hours at RT. 125µl of 0.01% Crystal violet solution (w/v) was added to each well and incubated in RT for 15 min. The plate was re-washed three times with water and then 125µl 30% Acetic acid (v/v) were added to each well. After 15 min incubation in RT, solutions in each well were transferred to a new 96 well plate. O.D. 550nm was used to measure biofilm formation, and O.D. 600nm for data normalization.

Fluorescence microscopy. Overnight cultures of cells with plasmids encoding fluorescent fusion proteins were diluted 1:100 in fresh M9M or LB medium with antibiotics and grown at 30°C with 0.02% arabinose for 4 hours (unless otherwise stated). For imaging cells, a cell suspension (5 µl) was applied to a slide and incubated for 5 min before imaging. Images were acquired using an Olympus BX53 microscope, appropriate filters, and cellSens standard software (version 1.6) from Olympus.

Gene alignment for identification of primary and secondary I-sites Primary I-site designation for YfiN was based on the identified a consensus RxxD, situated five amino acids upstream of the GGDEF catalytic site [12, 19, 58]. Secondary I-site designation for YfiN was predicted by comparing sequences from other DGCs that harbor experimentally identified secondary sites. Clustal Omega, available online (https://www.ebi.ac.uk/), was used for the prediction and alignment; DgcA was excluded from the analysis, because it has two predicted secondary I-sites.

For analysis of YfiN homologues, we used YfiN protein sequence of *E. coli* MG1655 from the UnitProt database (http://www.uniprot.org; accession number: P46139). Using UniRef50, we acquired 1974 orthologous sequences with minimum 50% sequence identity. Conservation of primary and secondary I-sites was calculated using the Clustal Omega tool.

Antibiotic survival assay on plates. An overnight culture of cYfiN strain was diluted 1:100 in M9M with or without IPTG. After 6 hours post-induction, cells were spread on agar plates containing either Ampicillin (20, 100 µg/ml), Gentamicin (10, 20 µg/ml) or Ciprofloxacin (1, 5µg/ml). After 12 hour incubation on these plates, cells were re-spread on fresh LB agar plates without antibiotics.

Antibiotic survival assay in liquid. An overnight culture of cYfiN strain was inoculated at 1:100 dilution in M9M. Cell cultures were grown for 2 hours to reach the OD_{600} of 0.1, at which IPTG was added. Two hours post-induction, either Gentamicin (20 µg/ml) or Ciprofloxacin (10µg/ml) was added. After a 4 hour treatment with antibiotics, cell cultures were washed with PBS buffer twice and plated on LB agar for CFU counts. The percent survival was calculated as follows: (final CFU/CFU before antibiotic treatment) × 100. The results are presented as the average results from at least 3 biological replicates.

Thin layer chromatography assay YfiN, YfiN I-site mutants (I_p, I_s, I_{ps}), and DgcA were induced from pBAD plasmids with arabinose in M9M for 3 hours. Then, cells were washed twice with PBS buffer and lysed with a VCX-750 Vibra-Cell sonicator at 20kHz (30 sec pulse followed by 10 sec cool-down for total of 5 cycles). Cell lysates were incubated with 1 mM GTP/[α-^{32}P]GTP (0.1 µCi/µl) (PerkinElmer) and incubated at 30°C for various time intervals for comparison pYfiN and pYfiN(Ips). Reactions were stopped by the addition of 1 volume of 0.5 M EDTA. Radio-labeled products were analyzed by polyethyleneimine-cellulose thin-layer chromatography (TLC; Millipore), by spotting 2 µl samples onto TLC plates. Plates were dried at RT for 5 min, and developed in 1.3 M KH_2PO_4 (pH 3.2) [12]. TLC data was analyzed with GE Typhoon Phosphorimager and ImageJ software by comparing the intensities of each blots on the TLC plate. GTP consumption was estimated based on the input GTP concentration.

GTPase assay. The GTP levels were measured using a GTPase-Glo Assay kit (Promega) which employs an ATP-linked luciferase reaction. Total concentration of GTP in cells was calculated based on the standard curve generated using a standard provided by manufacturer, and normalized to OD_{600} (OD_{600} 1.0 = 5x10^8 cells). The final concentration was represented

in ng/cell.

Metabolomics. *E. coli* MG1655 yfiR::kan pTrc99a-YfiN$_{GFP}$ (HK533) was grown at 30°C for 2 hours in 10 ml M9M, with IPTG for induction. Cells were incubated for additional 3 hours post-induction (OD_{600} reached around 0.4). Pellets were collected and flash frozen. They were shipped on dry ice to the Metabolomics Core Facility at the Mayo Clinic at Rochester, which routinely analyzes a panel of 219 commonly investigated metabolites such as dNTPs, NTPs, carbohydrates, and acids. We provided them with c-di-GMP, and they estimated these concentrations [59]. Samples were analyzed by high-performance liquid chromatography–tandem mass spectrometry (HPLC-MS/MS) at the facility, using a Thermo Fisher Q Exactive mass spectrometer. The analysis is qualitative, and data are provided as areas under elution peaks (AU, arbitrary unit). Of the 3 biological replicates sent to the Facility, one was unusable. COVID-19 work protocols during this time (August to Novemer, 2020), prevented us from sending more samples

Absolute quantification of the targeted nucleotides c-di-GMP and rNTPs was done by (HPLC-MS/MS) at the Metabolomics Core Facility at the University of Texas Medical Branch (UTMB). Cells were grown in M9M except with arabinose for induction. After 3.5 hours post-induction, cells were collected and their wet weight was measured for data normalization. Pellets were then flash frozen and mailed to UTMB. Three biological replicates for each set consisting $_{p}$Empty, $_{p}$YfiN, $_{p}$YfiN(I_{ps}), $_{p}$DgcA were prepared. The facility used ^{13}C-labeled standards to obtain a standard curve against which experimental values were derived.

Statistics. Unless mentioned otherwise, all the experiments were analyzed with unpaired t-test, p-value <0.001 ***, <0.01 **, and <0.5 **.

References

1. Galperin, M.Y., *Bacterial signal transduction network in a genomic perspective.* Environmental microbiology, 2004. **6**(6): p. 552-567.
2. Francis, V.I. and S.L. Porter, *Multikinase Networks: Two-Component Signaling Networks Integrating Multiple Stimuli.* Annual Review of Microbiology, 2019. **73**(1): p. 199-223.
3. Boor, K.J., *Bacterial stress responses: what doesn't kill them can make then stronger.* PLoS biology, 2006. **4**(1): p. e23-e23.
4. Fang, F.C., et al., *Bacterial Stress Responses during Host Infection.* Cell host & microbe, 2016. **20**(2): p. 133-143.
5. Ross, P., et al., *Regulation of cellulose synthesis in Acetobacter xylinum by cyclic diguanylic acid.* Nature, 1987. **325**(6101): p. 279-281.
6. Römling, U., M.Y. Galperin, and M. Gomelsky, *Cyclic di-GMP: the first 25 years of a universal bacterial second messenger.* Microbiology and molecular biology reviews : MMBR, 2013. **77**(1): p. 1-52.
7. Jenal, U., A. Reinders, and C. Lori, *Cyclic di-GMP: second messenger extraordinaire.* Nature Reviews Microbiology, 2017. **15**(5): p. 271-284.
8. Lori, C., et al., *Cyclic di-GMP acts as a cell cycle oscillator to drive chromosome replication.* Nature, 2015. **523**(7559): p. 236-239.
9. Tamayo, R., J.T. Pratt, and A. Camilli, *Roles of cyclic diguanylate in the regulation of bacterial pathogenesis.* Annual review of microbiology, 2007. **61**: p. 131-148.
10. Hoffman, L.R., et al., *Aminoglycoside antibiotics induce bacterial biofilm formation.* Nature, 2005. **436**(7054): p. 1171-5.
11. Suchanek, V.M., et al., *Chemotaxis and cyclic-di-GMP signalling control surface attachment of Escherichia coli.* Mol Microbiol, 2020. **113**(4): p. 728-739.
12. Christen, B., et al., *Allosteric Control of Cyclic di-GMP Signaling.* Journal of Biological Chemistry, 2006. **281**(42): p. 32015-32024.
13. Orr, M.W., et al., *A Subset of Exoribonucleases Serve as Degradative Enzymes for pGpG in c-di-GMP Signaling.* Journal of Bacteriology, 2018. **200**(24): p. e00300-18.
14. Hasegawa, K., S. Masuda, and T.-a. Ono, *Light Induced Structural Changes of a Full-length Protein and Its BLUF Domain in YcgF(Blrp), a Blue-Light Sensing Protein That Uses FAD (BLUF).* Biochemistry, 2006. **45**(11): p. 3785-3793.
15. Tuckerman, J.R., et al., *An oxygen-sensing diguanylate cyclase and phosphodiesterase couple for c-di-GMP control.* Biochemistry, 2009. **48**(41): p. 9764-74.
16. Jacob G. Malone , T.J., Pablo Manfredi,Andreas Dötsch,Andrea Blanka,Raphael Bos,Guy R. Cornelis,Susanne Häussler,Urs Jenal *The YfiBNR Signal Transduction Mechanism Reveals Novel Targets for the Evolution of Persistent Pseudomonas aeruginosa in Cystic Fibrosis Airways.* PLOS PATHOGENS, 2012. **8(6): e1002760.**
17. Walker, J.A., S. Rivera, and E.E. Weinert, *Mechanism and Role of Globin-Coupled Sensor Signalling.* Advances in microbial physiology, 2017. **71**: p. 133-169.

556 18. Zähringer, F., et al., *Structure and Signaling Mechanism of a Zinc-Sensory Diguanylate*
557 *Cyclase.* Structure, 2013. **21**(7): p. 1149-1157.
558 19. Wassmann, P., et al., *Structure of BeF3- -modified response regulator PleD: implications for*
559 *diguanylate cyclase activation, catalysis, and feedback inhibition.* Structure, 2007. **15**(8): p.
560 915-27.
561 20. Dahlstrom, K.M., et al., *The Inhibitory Site of a Diguanylate Cyclase Is a Necessary Element*
562 *for Interaction and Signaling with an Effector Protein.* J Bacteriol, 2016. **198**(11): p. 1595-
563 603.
564 21. Giardina G, P.A., Fernicola S, Franceschini S, Rinaldo S, Stelitano V, *Investigating the Allosteric*
565 *Regulation of YfiN from Pseudomonas aeruginosa: Clues from the Structure of the Catalytic*
566 *Domain.* PLoS ONE, 2013. **8(11): e81324**.
567 22. Ueda, A. and T.K. Wood, *Tyrosine Phosphatase TpbA of Pseudomonas aeruginosa Controls*
568 *Extracellular DNA via Cyclic Diguanylic Acid Concentrations.* Environ Microbiol, 2010. **2**(3): p.
569 449-55.
570 23. Jacob G. Malone , T.J., Christian Spangler,Daniel Ritz,Anne Spang,Cécile
571 Arrieumerlou,Volkhard Kaever,Regine Landmann,Urs Jenal, *YfiBNR Mediates Cyclic di-GMP*
572 *Dependent Small Colony Variant Formation and Persistence in Pseudomonas aeruginosa.*
573 PLOS PATHOGENS, 2010. **6(3): e1000804**.
574 24. Kim, H.K. and R.M. Harshey, *A Diguanylate Cyclase Acts as a Cell Division Inhibitor in a Two-*
575 *Step Response to Reductive and Envelope Stresses.* mBio, 2016. **7**(4): p. e00822-16.
576 25. Katharios-Lanwermeyer, S., et al., *The Diguanylate Cyclase YfiN of Pseudomonas aeruginosa*
577 *Regulates Biofilm Maintenance in Response to Peroxide.* J Bacteriol, 2022. **204**(1): p.
578 e0039621.
579 26. Egan, A.J. and W. Vollmer, *The physiology of bacterial cell division.* Ann N Y Acad Sci, 2013.
580 **1277**: p. 8-28.
581 27. Hengge, R., et al., *Systematic Nomenclature for GGDEF and EAL Domain-Containing Cyclic*
582 *Di-GMP Turnover Proteins of Escherichia coli.* Journal of bacteriology, 2015. **198**(1): p. 7-11.
583 28. Frankel, D., *Glycolysis*. Escherichia coli and Salmonella tiphymurium: Cellular and Molecular
584 Biology. 2., ed. F. Neidhardt. 1996. 189–196.
585 29. Nieto, V., et al., *Under Elevated c-di-GMP in Escherichia coli, YcgR Alters Flagellar Motor Bias*
586 *and Speed Sequentially, with Additional Negative Control of the Flagellar Regulon via the*
587 *Adaptor Protein RssB*, 2019. **202**(1): p. e00578-19.
588 30. Chan, C., et al., *Structural basis of activity and allosteric control of diguanylate cyclase.* Proc
589 Natl Acad Sci U S A, 2004. **101**(49): p. 17084-9.
590 31. Hauryliuk, V., et al., *Recent functional insights into the role of (p)ppGpp in bacterial*
591 *physiology.* Nature reviews. Microbiology, 2015. **13**(5): p. 298-309.
592 32. Diehl, F.F., et al., *Cellular redox state constrains serine synthesis and nucleotide production*
593 *to impact cell proliferation.* Nature Metabolism, 2019. **1**(9): p. 861-867.
594 33. Diehl, F.F., et al., *Nucleotide imbalance decouples cell growth from cell proliferation.* Nature

595 Cell Biology, 2022. **24**(8): p. 1252-1264.
596 34. Patil, P.R., et al., *A revised mechanism for (p)ppGpp synthesis by Rel proteins: The critical*
597 *role of the 2'-OH of GTP.* J Biol Chem, 2020. **295**(37): p. 12851-12867.
598 35. Kriel, A., et al., *Direct regulation of GTP homeostasis by (p)ppGpp: a critical component of*
599 *viability and stress resistance.* Molecular cell, 2012. **48**(2): p. 231-241.
600 36. Gaca, A.O., C. Colomer-Winter, and J.A. Lemos, *Many means to a common end: the intricacies*
601 *of (p)ppGpp metabolism and its control of bacterial homeostasis.* Journal of bacteriology,
602 2015. **197**(7): p. 1146-1156.
603 37. Ronneau, S. and R. Hallez, *Make and break the alarmone: regulation of (p)ppGpp*
604 *synthetase/hydrolase enzymes in bacteria.* FEMS Microbiology Reviews, 2019. **43**(4): p. 389-
605 400.
606 38. Bennett, B.D., et al., *Absolute metabolite concentrations and implied enzyme active site*
607 *occupancy in Escherichia coli.* Nature chemical biology, 2009. **5**(8): p. 593-599.
608 39. Granner, D. and S. Pilkis, *The genes of hepatic glucose metabolism.* J Biol Chem, 1990.
609 **265**(18): p. 10173-6.
610 40. Kohanski, M.A., D.J. Dwyer, and J.J. Collins, *How antibiotics kill bacteria: from targets to*
611 *networks.* Nature reviews. Microbiology, 2010. **8**(6): p. 423-435.
612 41. Sarenko, O., et al., *More than Enzymes That Make or Break Cyclic Di-GMP—Local Signaling*
613 *in the Interactome of GGDEF/EAL Domain Proteins of Escherichia coli.* mBio, 2017. **8**(5): p.
614 e01639-17.
615 42. Mitchell, A.M. and T.J. Silhavy, *Envelope stress responses: balancing damage repair and*
616 *toxicity.* Nat Rev Microbiol, 2019. **17**(7): p. 417-428.
617 43. Gresham D, D.M., Tucker CM, Jenq HT, Pai DA, Ward, *A The Repertoire and Dynamics of*
618 *Evolutionary Adaptations to Controlled Nutrient-Limited Environments in Yeast.* PLoS
619 Genetics, 2008. **4(12): e1000303.** https://doi.org/10.1371/journal.pgen.1000303.
620 44. Daignan-Fornier B, L.D.a.S., *Quiescence Through the Prism of Evolution.* Front. Cell Dev. Biol,
621 2021. **9:745069**(10.3389/fcell.2021.745069).
622 45. Moore, N. and S. Lyle, *Quiescent, slow-cycling stem cell populations in cancer: a review of*
623 *the evidence and discussion of significance.* J Oncol, 2011. **2011**.
624 46. Tchawa Yimga, M., et al., *Role of gluconeogenesis and the tricarboxylic acid cycle in the*
625 *virulence of Salmonella enterica serovar Typhimurium in BALB/c mice.* Infect Immun, 2006.
626 **74**(2): p. 1130-40.
627 47. Sauer, U. and B.J. Eikmanns, *The PEP—pyruvate—oxaloacetate node as the switch point for*
628 *carbon flux distribution in bacteria: We dedicate this paper to Rudolf K. Thauer, Director of*
629 *the Max-Planck-Institute for Terrestrial Microbiology in Marburg, Germany, on the occasion*
630 *of his 65th birthday.* FEMS Microbiology Reviews, 2005. **29**(4): p. 765-794.
631 48. Kuroda, A. and A. Kornberg, *Polyphosphate kinase as a nucleoside diphosphate kinase in*
632 *Escherichia coli and Pseudomonas aeruginosa.* Proceedings of the National Academy of
633 Sciences, 1997. **94**(2): p. 439-442.
634 49. Gaal, T., et al., *Transcription Regulation by Initiating NTP Concentration: rRNA Synthesis in*

Bacteria. Science, 1997. **278**(5346): p. 2092.
50. Visconti, A., et al., *Interplay between the human gut microbiome and host metabolism.* Nature Communications, 2019. **10**(1): p. 4505.
51. Fridman, O., et al., *Optimization of lag time underlies antibiotic tolerance in evolved bacterial populations.* Nature, 2014. **513**(7518): p. 418-421.
52. Bertrand, R.L., *Lag Phase Is a Dynamic, Organized, Adaptive, and Evolvable Period That Prepares Bacteria for Cell Division.* Journal of Bacteriology, 2019. **201**(7): p. e00697-18.
53. Sánchez-Romero, M.A. and J. Casadesús, *Contribution of phenotypic heterogeneity to adaptive antibiotic resistance.* Proceedings of the National Academy of Sciences, 2014. **111**(1): p. 355-360.
54. Adkar, B.V., et al., *Optimization of lag phase shapes the evolution of a bacterial enzyme.* Nature Ecology & Evolution, 2017. **1**(6): p. 0149.
55. Rolfe, M.D., et al., *Lag phase is a distinct growth phase that prepares bacteria for exponential growth and involves transient metal accumulation.* J Bacteriol, 2012. **194**(3): p. 686-701.
56. Madar, D., et al., *Promoter activity dynamics in the lag phase of Escherichia coli.* BMC Syst Biol, 2013. **7**: p. 136.
57. Datsenko, K.A. and B.L. Wanner, *One-step inactivation of chromosomal genes in Escherichia coli K-12 using PCR products.* Proceedings of the National Academy of Sciences, 2000. **97**(12): p. 6640-6645.
58. Hengge, R., *Principles of c-di-GMP signalling in bacteria.* Nature Reviews Microbiology, 2009. **7**(4): p. 263-273.
59. Spangler, C., et al., *A liquid chromatography-coupled tandem mass spectrometry method for quantitation of cyclic di-guanosine monophosphate.* Journal of Microbiological Methods, 2010. **81**(3): p. 226-231.
60. Amann, E., J. Brosius, and M. Ptashne, *Vectors bearing a hybrid trp-lac promoter useful for regulated expression of cloned genes in Escherichia coli.* Gene, 1983. **25**(2-3): p. 167-78.
61. Guzman, L.M., et al., *Tight regulation, modulation, and high-level expression by vectors containing the arabinose PBAD promoter.* J Bacteriol, 1995. **177**(14): p. 4121-30.
62. Kitagawa, M., et al., *Complete set of ORF clones of Escherichia coli ASKA library (a complete set of E. coli K-12 ORF archive): unique resources for biological research.* DNA Res, 2005. **12**(5): p. 291-9.

Acknowledgements

We thank Souvik Bhattacharyya for helpful discussions and Hyo Kyung Kim for her strains. This work was supported by NIH grant R35GM118085.

Main Figures

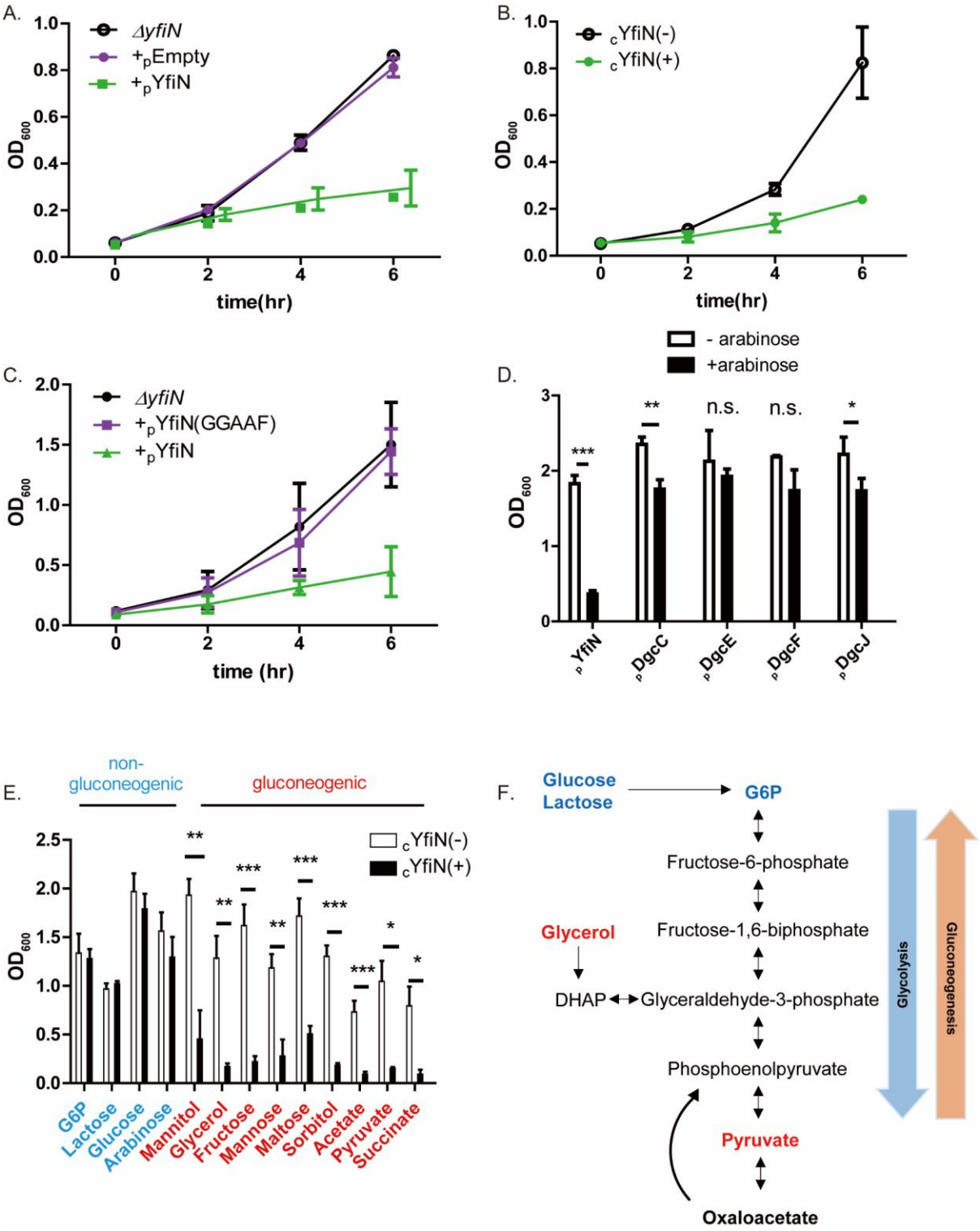

Figure 1. YfiN arrests *E. coli* growth only on specific carbon sources. *(A)* Time course of growth (OD_{600}) in M9 glycerol of Δ*yfiN E. coli* harboring either pYfiN or pEmpty (control) plasmids, where expression of *yfiN* is driven from the PBAD promoter (see Methods for media and arabinose inducer concentrations). *(B)* As *(A)*, except *yfiN* expression is from its chromosomal location ($cYfiN_{GFP}$), driven from the PTrc promoter. +/- indicate with or without IPTG addition. *(C)* As in *A*, except activity of pYfiN is compared with its active site mutant YfiN(GGAAF). *(D)* A panel of all five inner membrane DGCs of

E. coli (YfiN, DgcC, DgcE, DgcF, DgcJ) were cloned in the PBAD vector and expressed as in *A* for 12 hours prior to recording OD. (*E)* As in *B* (cYfiN)*,* except cells were grown in M9 media supplemented with indicated sugars, and OD_{600} measured at 8h. (*F*) Schematic of the gluconeogenesis and glycolysis pathways, with relevant metabolites color-coded as in *E*.

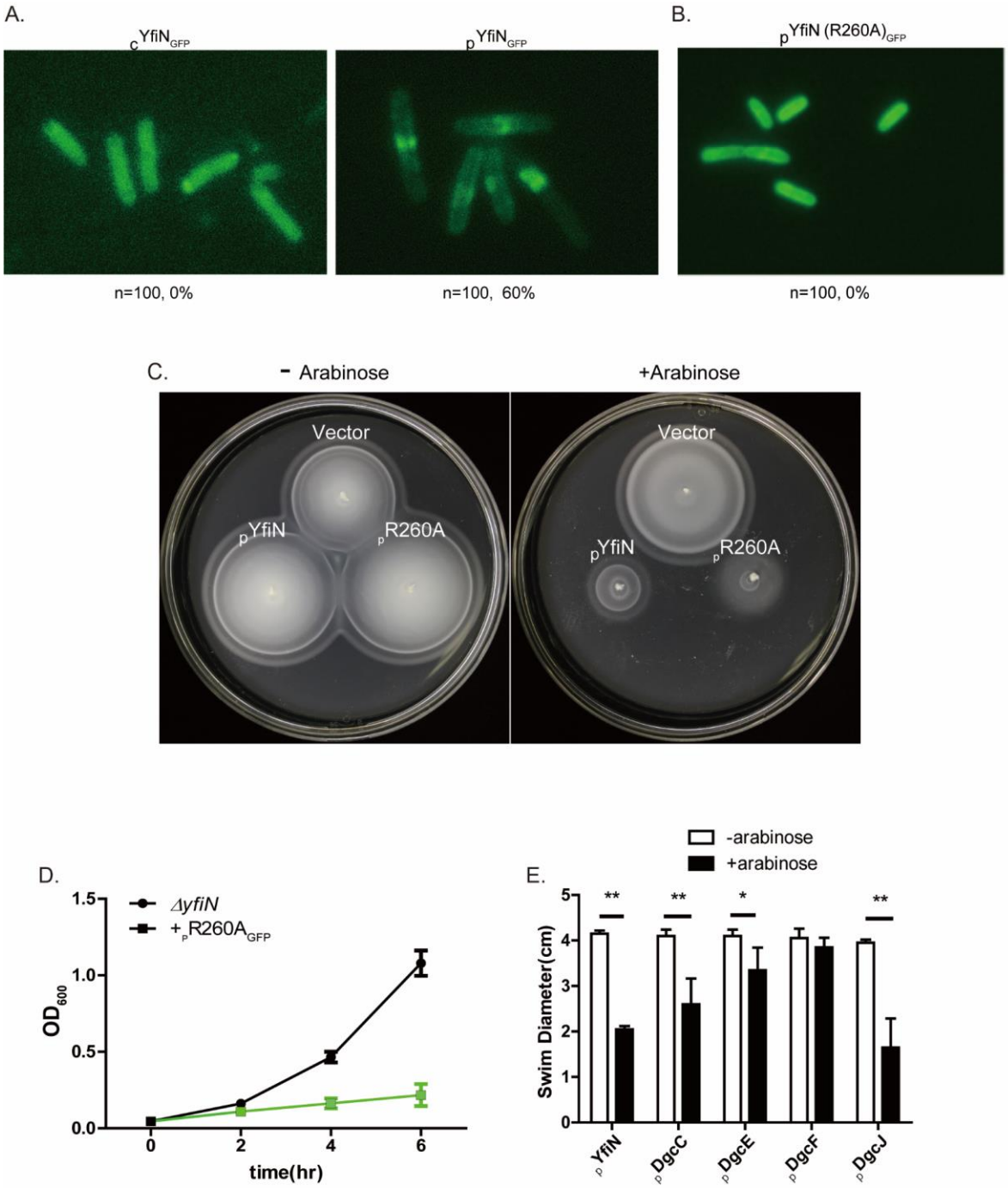

Figure 2. Growth-arrest phenotype of YfiN in M9 glycerol is independent of its relocation to the mid-cell. *(A)* Fluorescence images of $cYfiN_{GFP}$ and $pYfiN_{GFP}$ expressed for 4 hours in M9 glycerol media. The percentage of cells with $YfiN_{GFP}$ foci at the mid-cell is indicated, with n = total number of cells observed. *(B)* As in *A*, except with pYfiN $(R260A)_{GFP}$. *(C)* Motility of indicated strains (empty vector, $_pYfiN_{GFP}$, $_pYfiN(R260A)_{GFP}$ -/+ inducer in 0.3% soft agar plates,. *(D)* Growth curves of the indicated strains in M9 glycerol. (*E*) DGC activity of all 5 inner membrane DGCs of *E. coli* as measured by motility in soft agar.

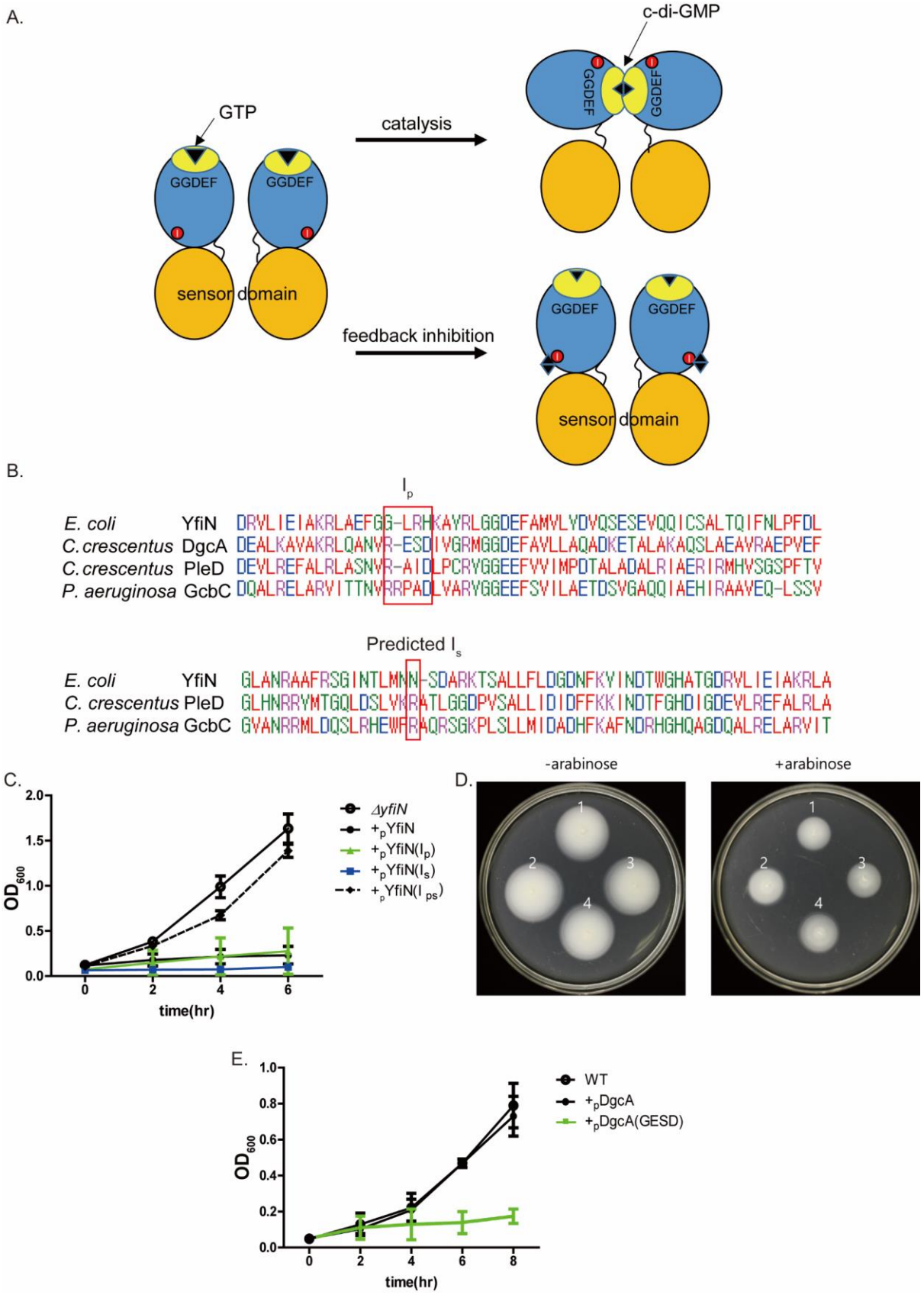

Figure 3. Growth arrest by YfiN is related to absence of autoinhibitory I sites. *(A)* Schematic of I-site mediated feedback inhibition. DGCs (dimer) sense environmental stimuli though their sensor domains (orange), and relay the signal to their catalytic domain to synthesize c-di-GMP. Upon reception of the sensory signal, GGDEF active sites (yellow) align in the dimer [7, 30] to produce c-di-GMP

(diamond) from 2 GTPs. Product inhibition occurs when c-di-GMP binds to I-sites, preventing the two active sites from interacting. (*B*) The primary (I_p) (RxxD) and predicted secondary (I_s) auto-inhibitory sites are boxed in a sequence alignment of various DGCs around these sites (see Methods). (*C*) Growth in M9 glycerol of pYfiN derivatives reconstituted for primary (Ip), secondary (Is) or both (Ips) I-sites. Expression was induced with arabinose. (*D*) Motility of indicated strains (1: pYfiN, 2: pYfiN I_p, 3: pYfiN I_s, 4: pYfiN I_{ps}) assayed in soft agar plates. (*E)* As in C, except with cells expressing DgcA and its mutant I_p site (RESD→GESD).

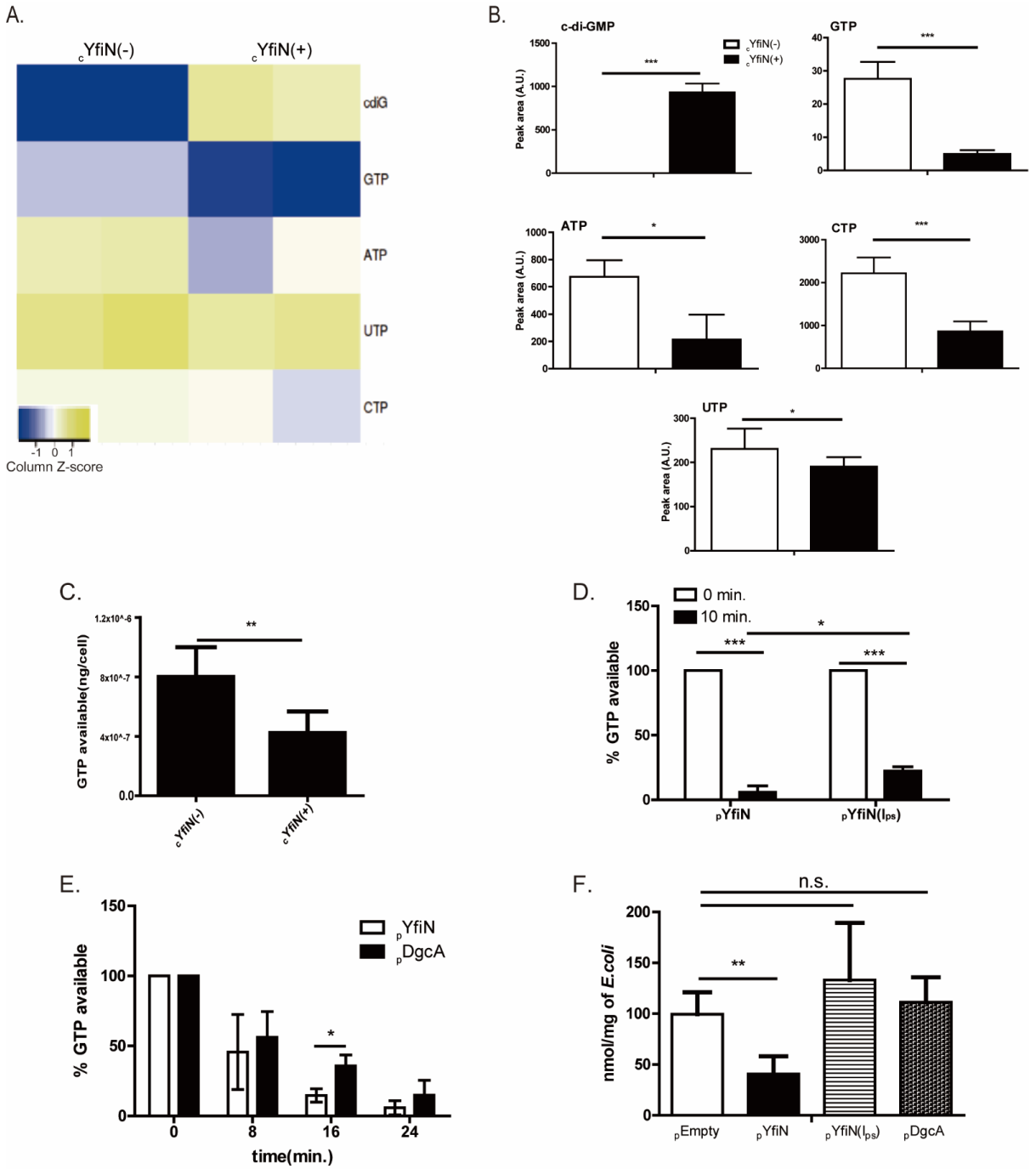

Figure 4. YfiN depletes intracellular GTP. (*A*) Metabolite profiling of cYfIN was performed using two replicates samples with and without inducer (+/-) (see Methods). Among ~219 metabolites measured using the targeted metabolomics approach, levels of c-di-GMP (cdiG) and the four ribonucleotides (GTP, ATP, UTP, CTP) are shown. Intensities of metabolites (log10 transformed) are displayed as a heatmap, each replicate occupying a square. *(B)* To measure the statistical significance of the estimates in A, the areas under the curve of eluted peaks were calibrated as AU (arbitrary units), and the data replotted as bar graphs. (*C*) A luciferase-based GTP assay kit was used to measure GTP levels (ng/cell) in lysates of YfiN-expressing cells 3 hours post-induction. (*D)* Lysates of M9 glycerol-grown cells expressing $_{p}$YfiN and $_{p}$YfiN I_{ps} were incubated with [α-32P] GTP for 5-minute intervals from 0-15 minutes, and analyzed using TLC (see Methods); only the 10 min data are shown (see text). Each replicate was normalized to initial GTP levels set at 100%. *(E)* As in *D,* but with lysates of cells expressing $_{p}$YfiN and $_{p}$DgcA. *(F)* Absolute quantification of GTP levels in cells expressing indicated plasmids (see Methods). Concentration of GTP for each biological replicate was normalized to wet weight of *E. coli* cells.

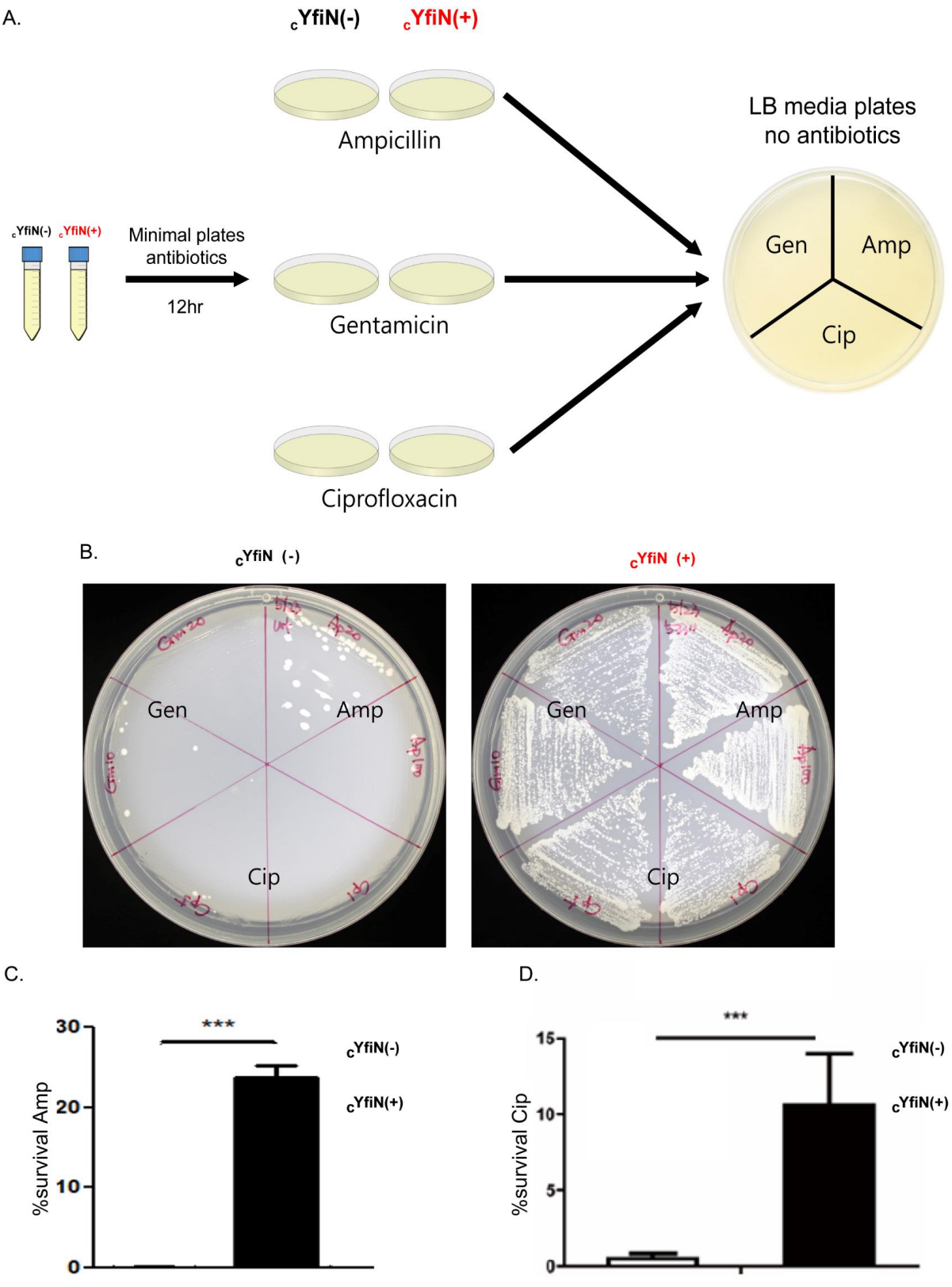

Figure 5. YfiN increases tolerance to different classes of antibiotics. *(A)* Experimental design. (cYfiN)-expressing cells grown with or without inducer (+/-) in liquid M9 glycerol media were plated on M9 glycerol plates supplemented with two different antibiotic concentrations: Ampicillin (Amp; 20 & 100ug/ml), Gentamicin (Gen; 4 & 20ug/ml), Ciprofloxacin (Cip; 2 & 10ug/ml). After overnight incubation, inoculating loops were used to transfer cells to fresh LB plates without antibiotics. The results are shown in *(B)*. Note that there are no antibiotics in the plates shown in B; the labels merely indicate the antibiotic they were treated with on the M9 plates prior to inoculation on the LB plates. *(C-D)* In a separate set of

experiments, cells grown with or without YfiN (cYfiN) in M9 glycerol liquid media for 3 hours were exposed to (*C*) Amp 100ug/ml or (*D*) Cip 10ug/ml) for 4 hours, before plating on LB. % survival under the three conditions was determined by measuring CFU counts before and after exposure to antibiotics.

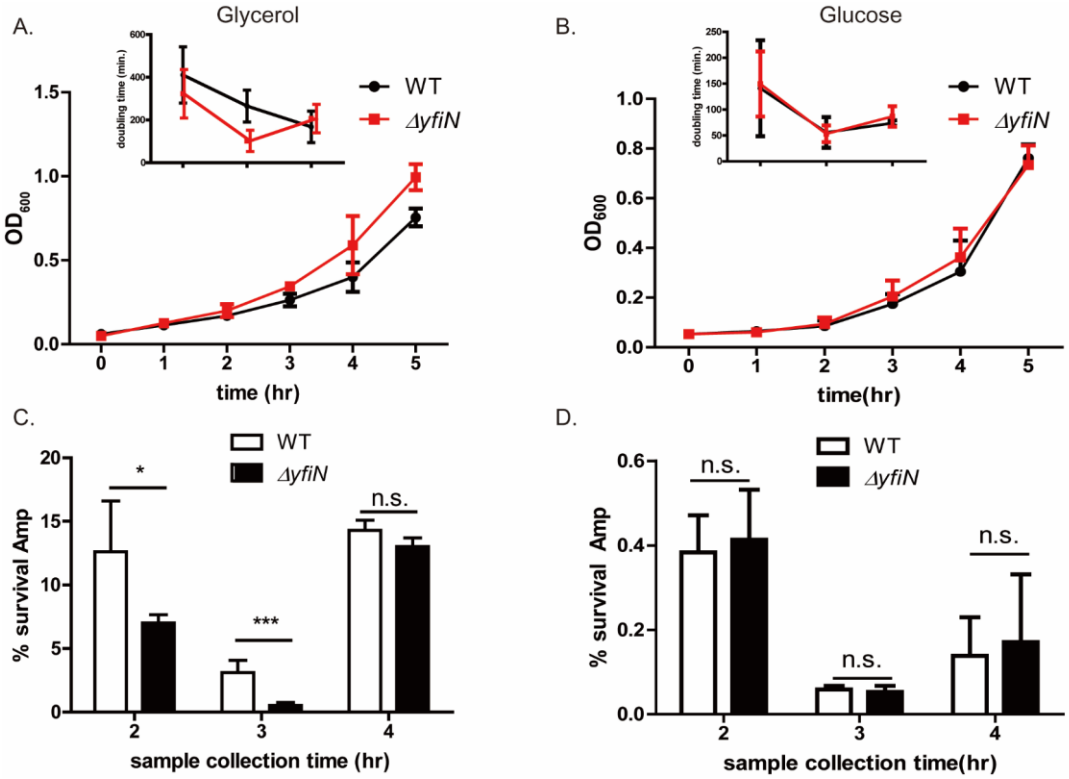

Figure 6. Native YfiN increases the duration of the lag phase of growth. (*A,B*) Growth of WT versus *ΔyfiN* strains in M9 glycerol or glucose. Insets show doubling time in minutes for the strains measured at 2-hour intervals during growth, each tick on the x-axis marking these intervals. (*C-D*) WT and *ΔyfiN* strains were grown in M9 glycerol or glucose for 0-4 hours and samples were collected at 2, 3 or 4 hours (x-axis), followed by treatment with 100µg/ml Ampicillin for an additional 4 hours. At each time, % survival was calculated by comparing CFU counts before and after antibiotic treatment.

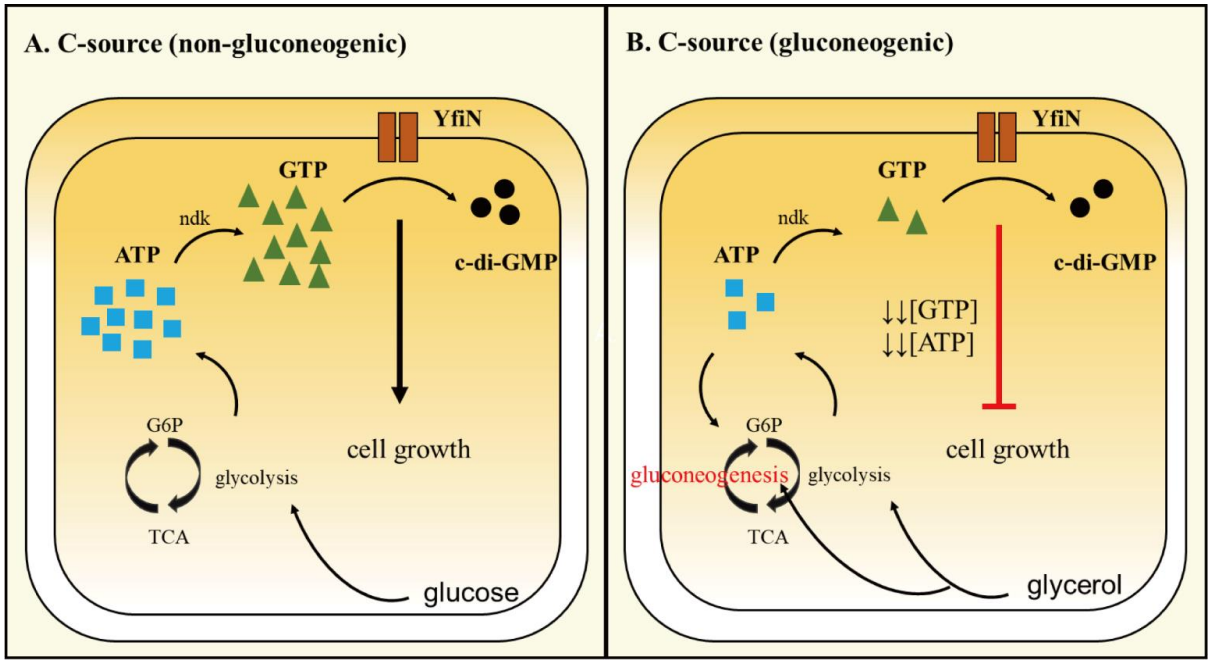

Figure 7. Model for mechanism of YfiN-mediated growth arrest on gluconeogenic carbon (C) sources. (*A*) On glycolytic substrates or rich media, GTP consumption by YfiN does not deplete NTP pools because they are abundant. (*B*) On non-gluconeogenic carbon sources NTP pools are low to begin with, and easily depleted by YfiN activity.

Supplementary Figures and Tables

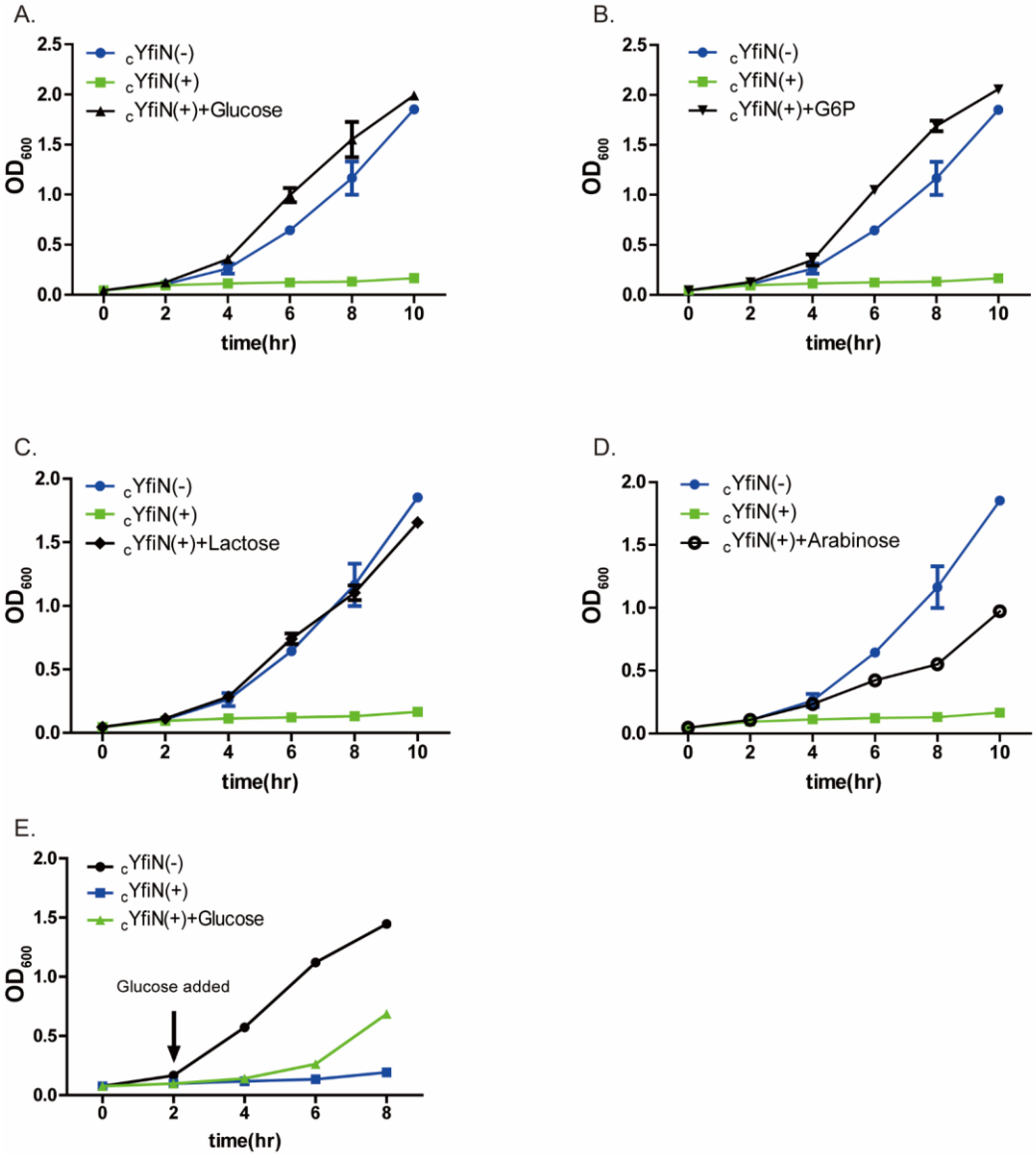

Figure S1. Glycolytic sugars rescue growth-arrest caused by gluconeogenic sugars. *(A-D)* Cells expressing cYfiN were propagated in glycerol (not indicated) or in combination with glycolytic substrates. *(E)* cYfiN was propagated in M9 glycerol, and glucose was added at 2 hours post induction. All substrates were at 0.2% w/v. Induction conditions as in Fig. 1.

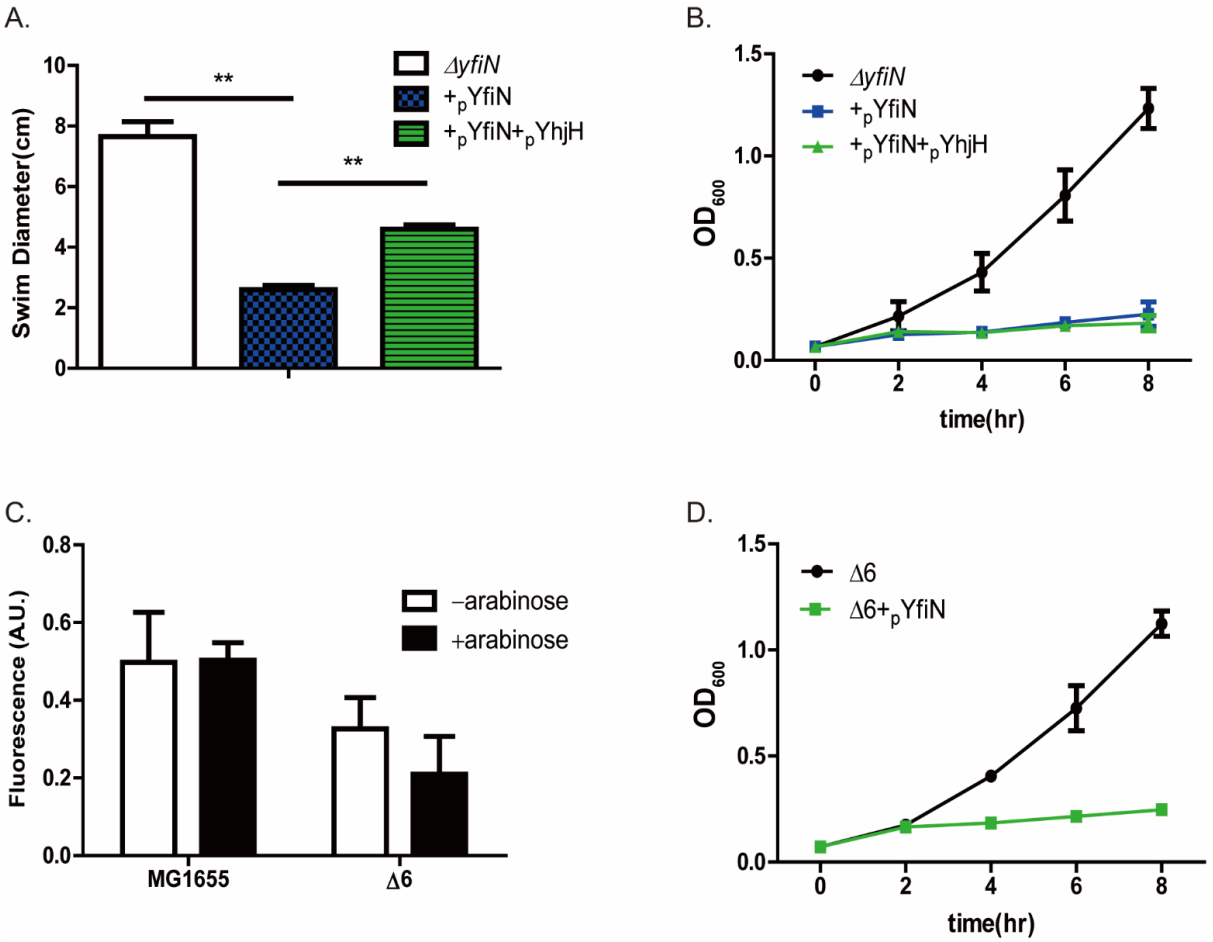

Figure S2. The growth-arrest phenotype of YfiN is unrelated to its motility or biofilm output. (*A*) pYfiN or pYfiN+pYhjH were introduced into the Δ*yfiN* strain and expression induced with arabinose, or arabinose+IPTG respectively. Motility was measured by estimating the diameter of the swim colony in soft agar plates. (*B*) Strains in *A* were monitored for growth in M9 glycerol in the presence of their respective inducers. (*C*) The parent MG1655 strain was deleted for six genes that control all the biofilm pathways in *E. coli* (Δ6 = *bcsA, csgD, pgaC, fimA, wcaD, yjbE*). pYfiN was introduced in both strains and the amount of biofilm formed was estimated by Crystal violet staining with or without arabinose in 96 well plates. A.U., arbitrary fluorescence units. (*D*) Strains in *C* were monitored for growth in M9 glycerol in the presence of arabinose.

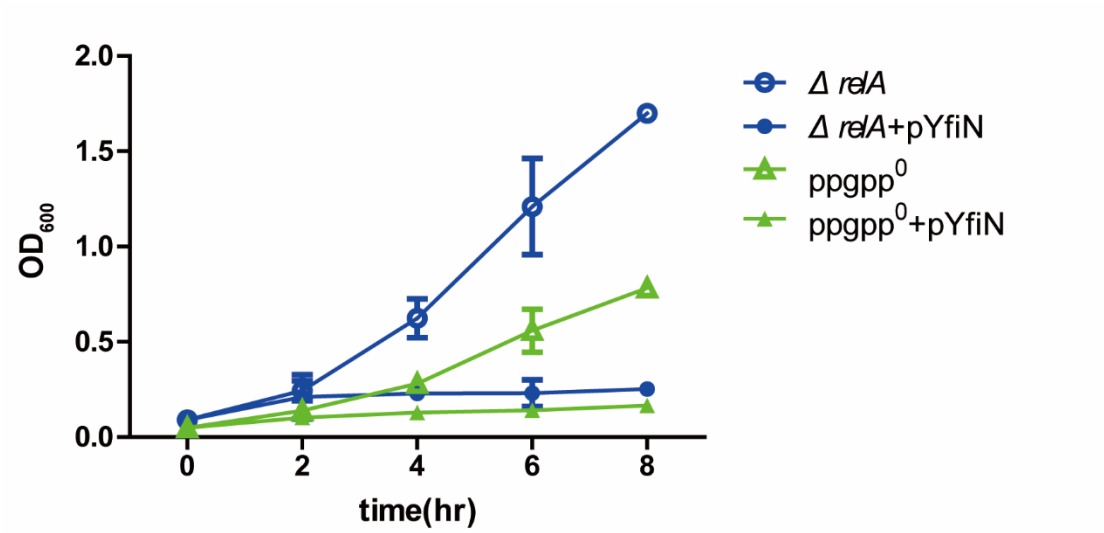

Figure S3. The (p)ppGpp pathway does not contribute to YfiN-mediated growth arrest. *ΔrelA* or *ΔrelAΔspoT*(ppGpp^0) strains were transformed with pYfiN in M9 glycerol and the time course of growth monitored.

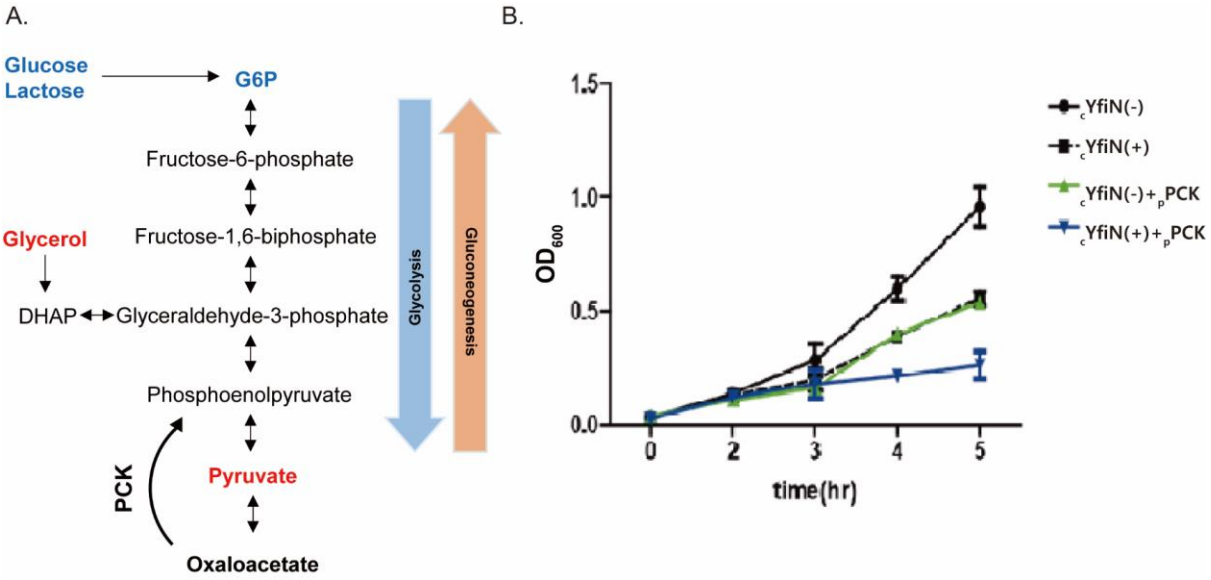

Figure S4. Co-expression of PCK with YfiN increases severity of growth arrest. *(A)* Gluconeogenesis pathway indicating the step at which PCK acts. *(B)* Growth curve in M9 mannitol of the $_{c}$YfiN strain transformed with pPCK.

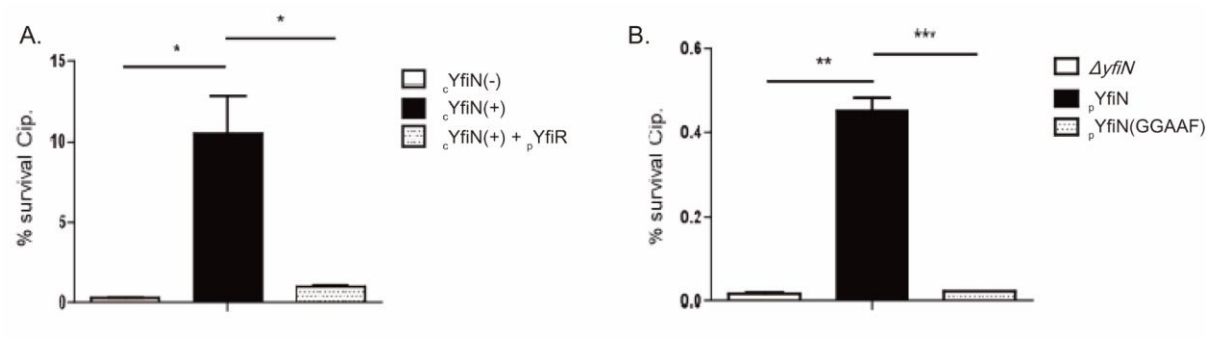

Figure S5. The DGC activity of YfiN is essential for antibiotic tolerance. (*A*) The cYfiN strain was transformed with pYfiR (periplasmic inhibitor of YfiN) and induced with IPTG or arabinose, respectively. Cells were propagated in M9 glycerol for 4 hours before addition of Cip (20µg/ml) to the media. After incubation for 4 hours, % survival was determined by measuring CFU counts before and after antibiotic exposure. (*B*) As in *A* except with different plasmids. The lower cell survival in B vs A is likely due to higher GTP depletion in pYfiN compared to cYfiN.

		I_s					I_p									Active site				
PleD(C.crescentus)	K	R	A	T	···	R	A	I	D	L	P	C	R	Y	G	G	E	E	F
YfiN(Y.frederiksenii)	K	D	C	-	···	R	E	S	D	L	V	A	R	L	G	G	D	E	F
YfiN(Y.intermedia)	S	D	C	-	···	R	E	T	D	L	V	A	R	L	G	G	D	E	F
YfiN(P.fluorescens)	R	S	A	A	···	R	E	D	D	L	V	A	R	L	G	G	D	E	F
YfiN(P.aeruginosa)	R	D	A	N	···	R	E	S	D	L	V	A	R	L	G	G	D	E	F
Consensus		R				R	X	X	D						G	G	D	E	F

Figure S6. YfiN homologs that have I_p but not I_s sites. The I_p site (RXXD), the predicted I_s site (R), and the DGC active site (GGDEF) are boxed in a sequence alignment of YfiN from *Yersinia* (Y) and *Pseudomonas* (P) species, and compared to PleD from *C. crescentus*, which has a functional set of both I sites (see Fig. 3B).

Table S1. Strains and Plasmids

Strains,	Genotype or Description	Reference
MG1655	K12 wild-type (WT) strain: F^- , λ^- , rph-1	Laboratory Collection
HK359	Δ*yfiN* in MG1655	[24]
HK461	HK359 + pBAD30_YfiN$_{GFP}$	[24]
JH101	HK359 + pBAD30_YfiN	This study
HK532	MG1655 yfiR::kan(←) yfiN::pBAD-*yfiN-gfp*	[24]
HK533	MG1655 yfiR::kan(←) yfiN::pTrc-*yfiN-gfp*	This study
JH102	MG1655 + pBAD33_DgcA	This study
JH100	HK359 + pBAD30_YfiN	This study
JH103	HK359 + pBAD30_YfiN(GGAAF)	This study
JH104	HK359 + pBAD30_YfiN(I_p)	This study
JH105	HK359 + pBAD30_YfiN(I_s)	This study
JH106	HK359 + pBAD30_YfiN(I_{ps})	This study
JH107	MG1655 + pBAD33_DgcA(GESD)	This study
JH108	HK359 + pBAD33_YfiN(R260A)$_{GFP}$	This study
JH109	HK532 + ASKA_PCK	This study
JH202	MG1655 + pBAD33_DgcC	This study
JH203	MG1655 + pBAD33_DgcE	This study
JH204	MG1655 + pBAD33_DgcF	This study
JH201	MG1655 + pBAD33_DgcJ	This study
JP1932	AW405 Δ*bcsA csgD pgaC fimA wcaD yjbE*	[29]
JH110	HK532 + pTrc99a_YhjH	This study
JH111	HK532 + pTrc99a_YfiR	This study
Plasmids	**Expressed Proteins**	**Reference**
pKD4	Kanamycin resistance gene template	[57]
pKD46	λ Red Recombinase	[57]
pCP20	FLP recombinase	[57]
pTrc99a	Cloning vector, P_{Trc}; Amp^R	[60]
pBAD30	Cloning vector; P_{BAD}; Amp^R	[61]

pBAD33	Cloning vector; P_{BAD}; Cm^R	[61]
pBAD30_YfiN$_{GFP}$	pBAD::YfiN-GFP(C-terminal)	[24]
pBAD30_YfiN	pBAD::YfiN	This study
pBAD30_YfiN(GGAAF)	pBAD:: YfiN (D329A E330A)	This study
pBAD30_YfiN(Ip)	pBAD::YfiN (G317R H320D)	This study
pBAD30_YfiN(Is)	pBAD::YfiN (N280R)	This study
pBAD30_YfiN(Ips)	pBAD::YfiN (N280R G317R H320D)	This study
pBAD33_DgcA	pBAD::DgcA	This study
pBAD33_DgcA(GESD)	pBAD::DgcA (R80G)	This study
pBAD30_YfiN(R260A)$_{GFP}$	pBAD::YfiN (R260A)-GFP	This study
pBAD33_DgcC	pBAD::DgcC	This study
pBAD33_DgcE	pBAD::DgcE	This study
pBAD33_DgcF	pBAD::DgcF	This study
pBAD33_DgcJ	pBAD::DgcJ	This study
pTrc99a_YhjH	pTrc::YhjH	This study
pTrc99a_YfiR	pTrc::YfiR	This study
ASKA_PCK	pASKA_PCK	[62]